


Spring 2019

Ruthenium-Catalyzed Ring-Opening/Ring-Closing Metathesis Polymerization

Christopher Elkhall

Follow this and additional works at: https://pilotscholars.up.edu/hon_projects

 Part of the [Biochemistry Commons](#), [Computer Sciences Commons](#), [Molecular Biology Commons](#), and the [Other Chemistry Commons](#)

Citation: Pilot Scholars Version (Modified MLA Style)

Elkhall, Christopher, "Ruthenium-Catalyzed Ring-Opening/Ring-Closing Metathesis Polymerization" (2019). *Honors Projects*. 38.

https://pilotscholars.up.edu/hon_projects/38

This Project is brought to you for free and open access by the Honors Program at Pilot Scholars. It has been accepted for inclusion in Honors Projects by an authorized administrator of Pilot Scholars. For more information, please contact library@up.edu.

Christopher Elkhall

Dr. Taylor

Chm 493

Spring 2019

Research Paper for Spring 2019

Abstract:

Polymerization reactions, which create a repeating chain of subunits, are crucial in the development and understanding of many essential materials and biological molecules. This research focuses on the mechanism of a polymerization reaction of monomers containing a cycloalkene and alkyne, which rearrange into a diene subunit under the influence of a ruthenium-based catalyst. This research examines why some monomers successfully polymerize while other similar monomers fail. Computational chemistry techniques (density functional theory) are used to study the mechanism and reactivity of each monomer. Our results show that the productive polymerization reaction competes with a side-reaction in which the catalyst reacts only with the alkyne, shutting down polymerization. A general model has been developed from the results to predict the reactivity of monomers based on the molecular geometry.

Introduction:

Synthesis of large organic compounds is often difficult because the compounds of interest are often very complex with many functional groups. Methods that form C=C bonds in selective ways are very valuable. One of the best-known ways to form a C=C bond is through the well-established olefin metathesis reaction which uses a transition-metal catalyst to alter certain double bonds in molecules to attach them to one another (Park et al., 2016). Being so widely studied, the reactivity and selectivity of such reactions can be fine-tuned for a product.

One way in which these catalysts may be implemented is through a polymerization mechanism. Polymerization is the process in which many singular small molecules, monomers, are chemically bonded together in a chain like fashion, so the resulting polymer will be a long chain of monomers. This process can occur with a singular monomer or more than one different monomer compound. A useful mechanism to carry out polymerization is through the use of a catalyst. The catalyst bonds to two monomers and chemically bonds them together. It will then detach from the monomers but continually bond one monomer at a time to this growing polymer chain.

Tandem olefin metathesis reactions have been developed, in which two or more reactions occur with the same catalyst within a single step. One main form of new study being done with tandem olefin metathesis is into the field of polymerization (Park et al., 2016). This uses a single monomer and a Grubbs catalyst to create a polymer chain consisting of many singular monomers strung together through formed C=C bonds.

The Choi research group has specifically developed a polymerization reaction that utilizes a succession of ring opening and ring closing metathesis reactions with the specific Grubbs 3 catalyst as shown in figure 1 below. It contains a SIMes ligand which stabilizes the catalyst. The

phenyl group begins all polymer chains. The two pyridine ligands dissociate in solution and expose the active site of the ruthenium and carbon double bond. The two chlorines also serve as stabilizing forces for the ruthenium center.

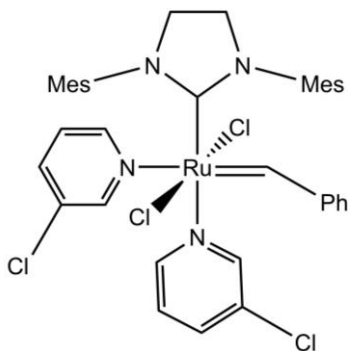


Figure 1. The Grubbs third generation catalyst.

The catalyst functions by continuously using tandem olefin metathesis reactions while moving down a chain of monomers to create the polymer outcome. Research is currently being done on monomers that include two main regions of interest, a cycloalkene and a terminal alkyne region indicated in Figure 3 below. The monomer in Figure 2 contains a generic X atom assignment in place of the changing linker group that binds the two sections of the monomer together.

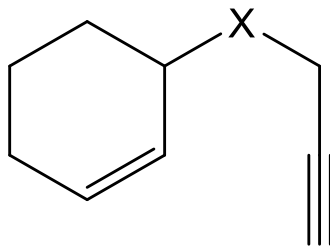


Figure 2. The monomeric subunit being used in the tandem olefin metathesis reaction.

By using this catalyst in presence of a monomer, the reaction will take place. The polymerization pathway is primarily divided into three main steps as shown in Figure 3 below. First, there is an initiation step in which monomer (1) binds to the catalyst quickly forming a four-membered ring with the alkyne of the monomer. The four-membered ring will then quickly rearrange so that the catalyst will now be bound to the monomer, forming (3). The product of this reaction is a simple ethylene molecule that remains in solution. In following a polymerization pathway, the catalyst of compound (3) will then form a complex with the cycloalkene portion of the monomer forming compound (4). The ruthenium will then initiate (TS5) by binding to the cycloalkene and forming a four membered ring as shown in (6). (TS7) follows when the four membered ring rearranges forming compound (8). This compound is then free to bind to another monomer in solution and restart the polymerization cycle. At any point in time during the life of compound (3), instead of forming a complex with the cycloalkene and continuing to polymerize, (3) can bind to the alkyne portion of a second monomer (1), forming (TS9) which quickly rearranges to form a stable compound (10) which will no longer be able to continue in the reaction. This deactivates the catalyst and renders any continuation of the reaction unattainable.

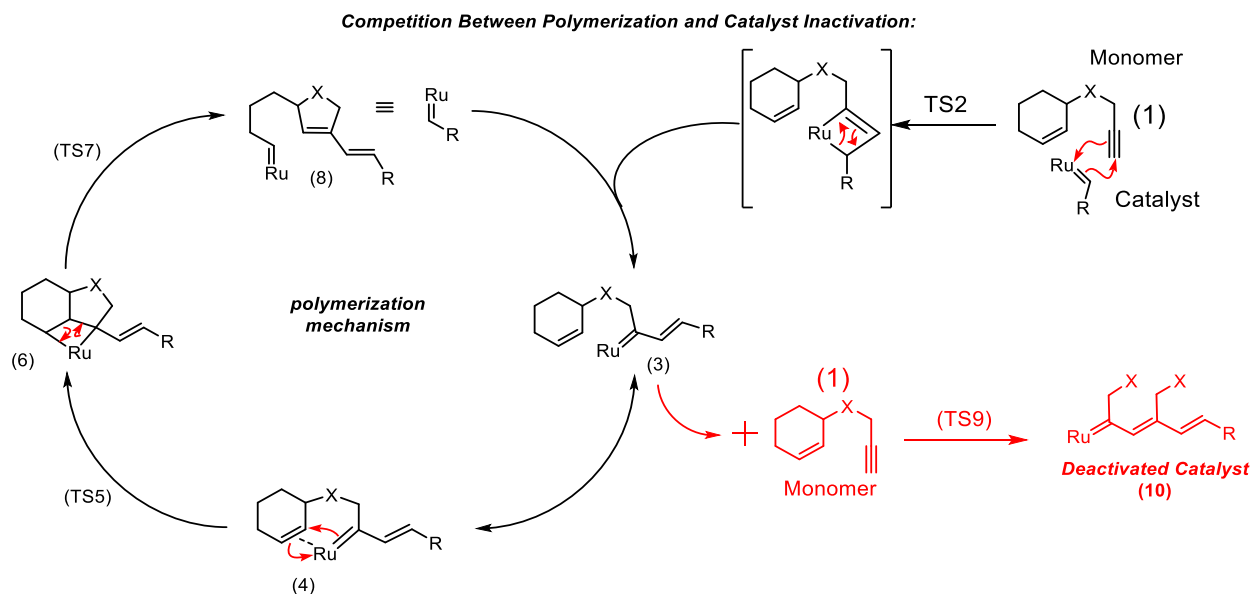


Figure 3. Ruthenium-catalyzed ring-opening/ring-closing metathesis polymerization mechanism and competing side chain deactivation pathway.

Experimental data seems to suggest that some monomers react with the catalyst, while others seem to react very poorly or not at (Park et al. 2013 and Park et al. 2016). Previous research has shown that by modifying the monomers using the Thorpe-Ingold effect as well as modifying the concentration of the catalyst there has been an increase in the reactivity of the unreactive monomers (Park et al. 2016). Still the question of why some monomers are extremely reactive while others do not react remains unclear. This research hopes to reach a better understanding of why such problems occur with certain monomers and not others.

This research will use density functional theory and other computational chemistry methods to further understand this polymerization reaction and the steps involved that initiate, propagate, and terminate this reaction. In the end, a detailed insight will be expressed about the reaction and how to manipulate the reaction in order to produce a certain outcome. This computational study will be further verified with experimental testing in order to verify its accuracy.

Methods:

DFT calculations were performed with Gaussian 09. Computed structures are illustrated using CYLView.

Geometries were optimized the B3LYP functional in the gas phase, using a mixed basis set of LANL2DZ (with ECP) for Ru and 6-31G(d) for all other atoms. Thermal corrections were calculated from unscaled vibrational frequencies at the same level of theory using a standard state of 298.15 K and 1 mol/L.

Gibbs free energies in Gaussian were calculated at the default pressure of 1 atm and corrected to the standard state in solution, 1 mol/L. The correction was made by adding $RT \ln(c_{\text{soln}}/c_{\text{gas}})$, or about 1.84 kcal/mol, to the free energy of all structures, where c_{soln} is the standard molar concentration in solution (1 mol/L) and c_{gas} is the standard molar concentration in the gas phase (0.0446 mol/L).

Electronic energies were obtained from single point energy calculations performed with the M064 functional and a mixed basis set of SDD for Ru and 6-311+G(d,p) for all other atoms. The SMD5 solvation model for n-octanol was used in M06 single point energy calculations.

Results and Discussion:

Energy, enthalpy, and Gibbs free energy values were calculated when the compounds were in gas (B3LYP) and were calculated when in the presence of a solution (MO6). These values were then calculated the change in units of kcal per mol using equation 2 below. Compound (4) of each reaction was used as the reactant measurement. This determined the necessary amount of energy, enthalpy, and Gibbs free energy required to acquire this monomeric step of each reaction based on the initial energy of compound (4).

$$[(TS) - (\Sigma \text{ reactants})] * 627.5095$$

Equation 1. Calculating the change in energy, enthalpy, and gibbs free energy and converting to kcal/mol.

Six different monomers were tested completely in this project. They are based on previous experimental results found by the choi group and they are depicted below in Figure 4.

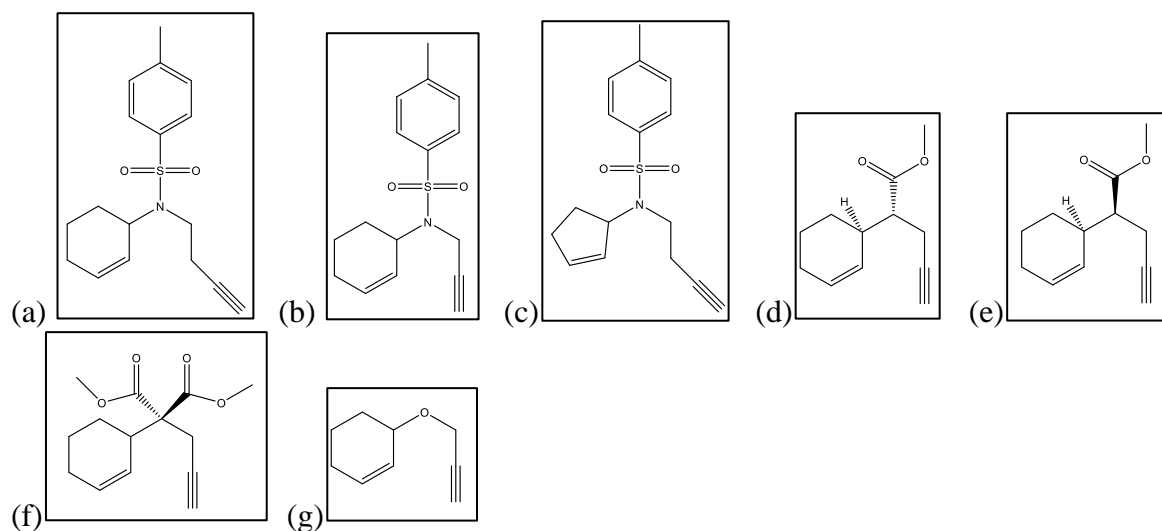


Figure 4. The monomers that have been tested. The monomers are the 66-Linker, the 65-Linker, the 56-Linker, the Two Ester Linker, the S conformer of the One Ester Linker, the R conformer of the One Ester Linker, and the Oxygen Linker from left to right or from labels a to g respectively.

The first monomer to be tested was the 65-Linker. This linker is known as the epitome of any reactions having a completion rate of 100% conversion in under 1 minute at room temperature (Park et al., 2013). The reaction conditions and results were further supported through the computational results depicting a very fast reaction based on the free energy required values displayed in Table 1 below. The reaction required 13.4 kcal/mol of free energy to overcome the activation energy required for the polymerization pathway to continue successfully. Along with the low energy required for the reaction, the deactivation pathway was greatly hindered comparatively to the polymerization pathway, having a required energy value of 15.8 kcal/mol. The difference of 2.4 kcal/mol for the deactivation pathway compared to the polymerization pathway means that the reaction will always follow the polymerization mechanism and never create a deactivated catalyst. These results indicate an extremely fast reaction based on the low energy barrier for polymerization along with a complete conversion based on the large difference between polymerization and deactivation. A visual depiction of the results is shown below in Figure 5.

Table 1. The change in energy, enthalpy, and Gibbs free energy of the 65-Linker. All values are given in kcal/mol.

Step of Reaction	ΔE	ΔH	ΔG
3	10.3	9.2	5.4
4	0.0	0.0	0.0
TS5	5.7	5.3	6.8
6	5.3	5.6	5.4
TS7	14.0	12.8	13.4
8	7.5	6.7	5.3
TS9	6.2	6.4	15.8

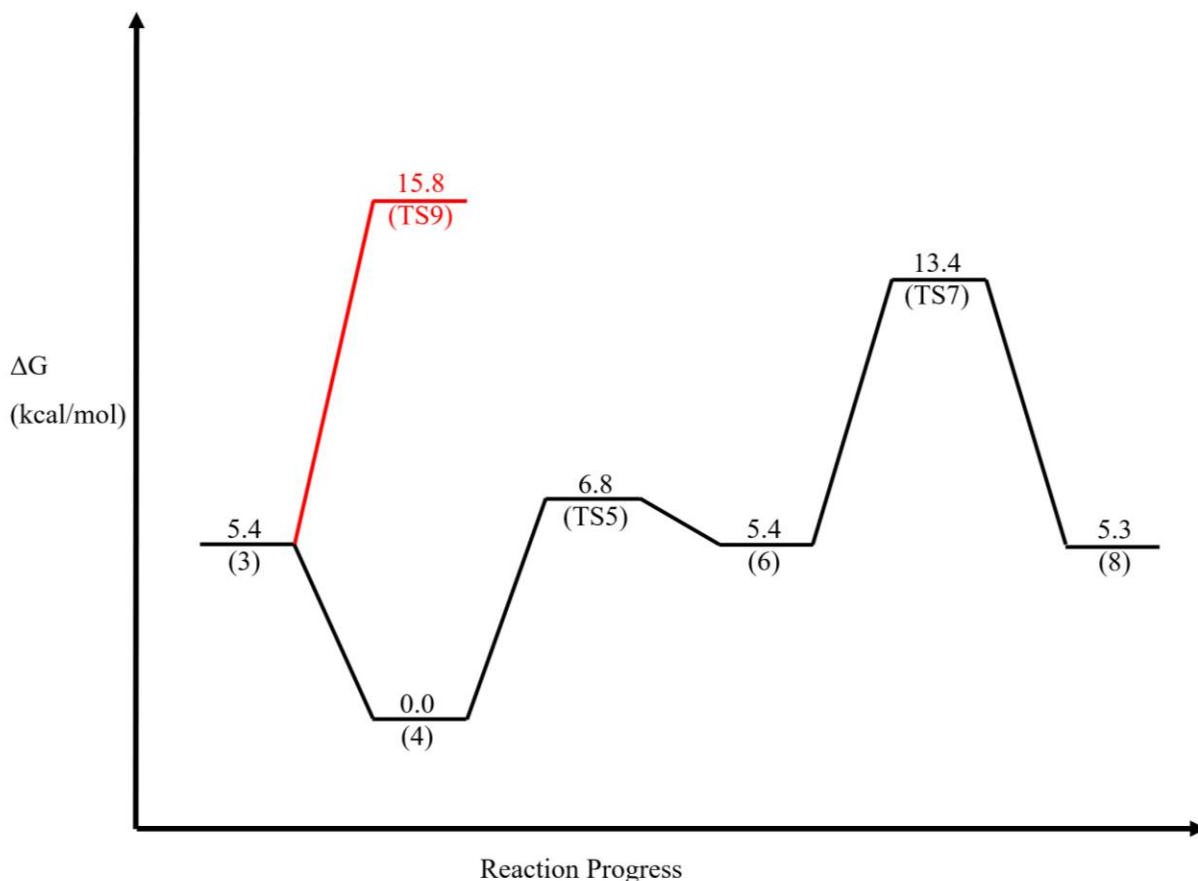


Figure 5. Visual reaction coordinate diagram for the 65-Linker.

The second monomer tested was the 66-Linker. This monomer seemed to be extremely similar to the 65-Linker and the same results were expected, but the experimental results seemed to differ along with the computational results from what was initially expected. The experimental results displayed a reaction of only 30% conversion at room temperature after a lengthy 12 hours (Park et al., 2013). This meant an extremely slow reaction or low yield reaction. The computational results that were found only slightly supported the experimental results in this case. The results indicated that it would be a very low yield reaction or no reaction because of the competitive pathways. The computational results displayed in Table 2 below, indicate a very small energy difference between the two reaction pathways. The barrier for entry for deactivation was found to

be only 8.7 kcal/mol versus the barrier for polymerization at 9.3 kcal/mol. The difference being only -0.6 between polymerization and deactivation, meaning both reactions will take place; although, deactivation does win the battle in most cases. Since both reactions are taking place the conversion of the reaction in total will be very low or results in no reaction because there is a relatively high probability that the catalyst will become deactivated at any one point in time. This does not perfectly support the experimental results indicating that no reaction will proceed computational versus a very slow reaction indicated experimentally. A visual depiction of the results is shown below in Figure 6.

Table 2. The change in energy, enthalpy, and Gibbs free energy of the 66-Linker. All values are given in kcal/mol.

Step of Reaction	ΔE	ΔH	ΔG
3	1.2	0.6	-1.1
4	0.0	0.0	0.0
TS5	7.1	6.7	9.3
6	4.9	5.2	6.9
TS7	7.9	7.0	8.6
8	4.2	3.6	3.9
TS9	-1.2	-0.9	8.7

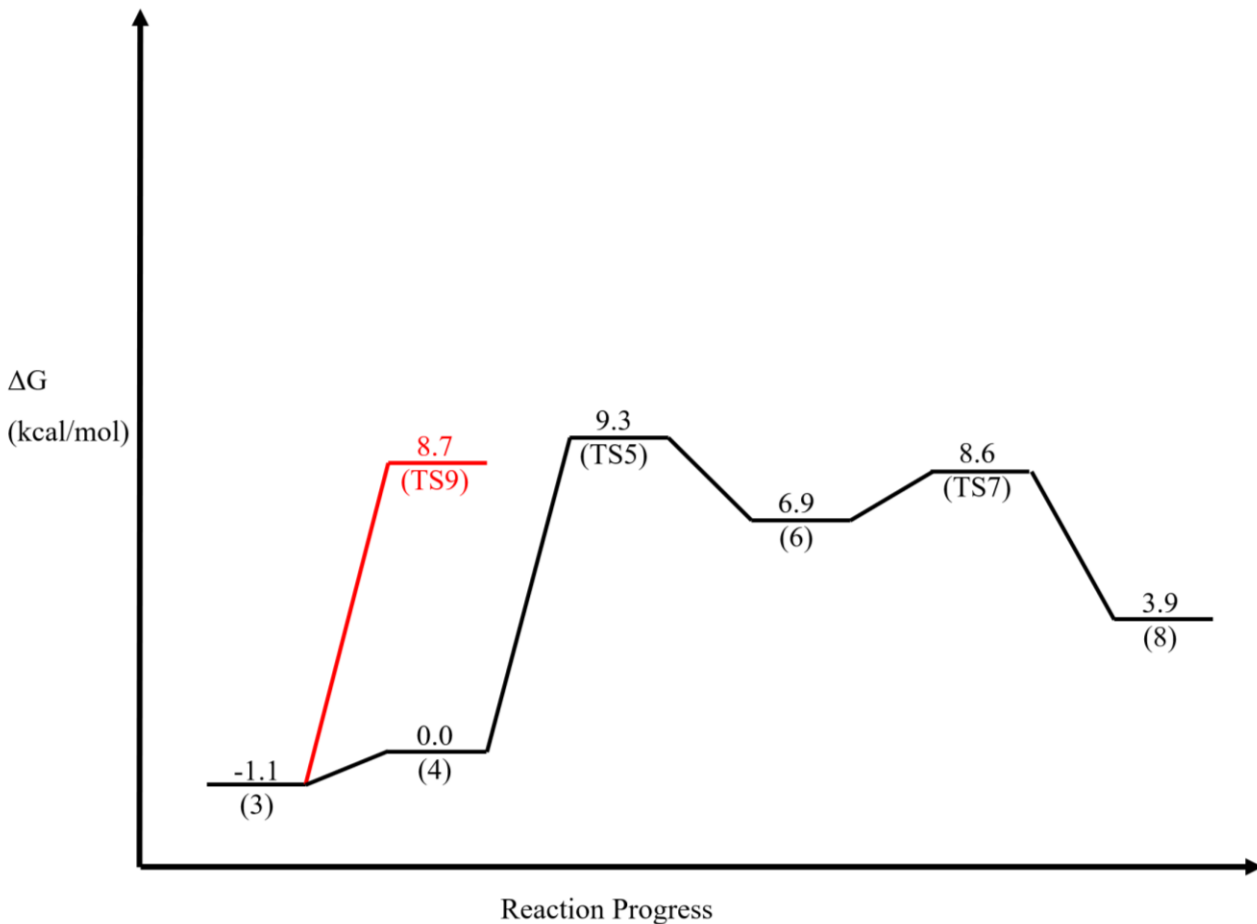


Figure 6. Visual reaction coordinate diagram for the 66-Linker.

The third monomer was the 56-Linker having experimental results of 80% conversion in 12 hours (Park et al., 2013). The computational results shown in Table 3 supported the experimental results in this case indicating a moderate to slow reaction based on the computational results. The computational results resulted in a relatively close deactivation and polymerization pathway required free energy values. The polymerization required about 9.1 kcal/mol versus the deactivation pathway which resulted in a 10.3 kcal/mol barrier of activation. The difference being about 1.2 kcal/mol for the reaction indicated that polymerization will outcompete the deactivation pathway in most cases, but the deactivation pathway will be followed a little bit of the time; however, polymerization does overcome deactivation in most

cases resulting in a moderate to slow reaction expected. This coincides with the experimental results found having a moderate reaction of 80% conversion in solution at room temperature after 12 hours of time. A visual representation of the computational results is shown below in Figure 7.

Table 3. The change in energy, enthalpy, and Gibbs free energy of the 56-Linker. All values are given in kcal/mol.

Step of Reaction	ΔE	ΔH	ΔG
3	6.2	5.6	3.4
4	0.0	0.0	0.0
TS5	4.5	5.0	9.1
6	-1.1	-0.8	2.1
TS7	3.5	2.8	5.7
TS9	1.2	1.6	10.3

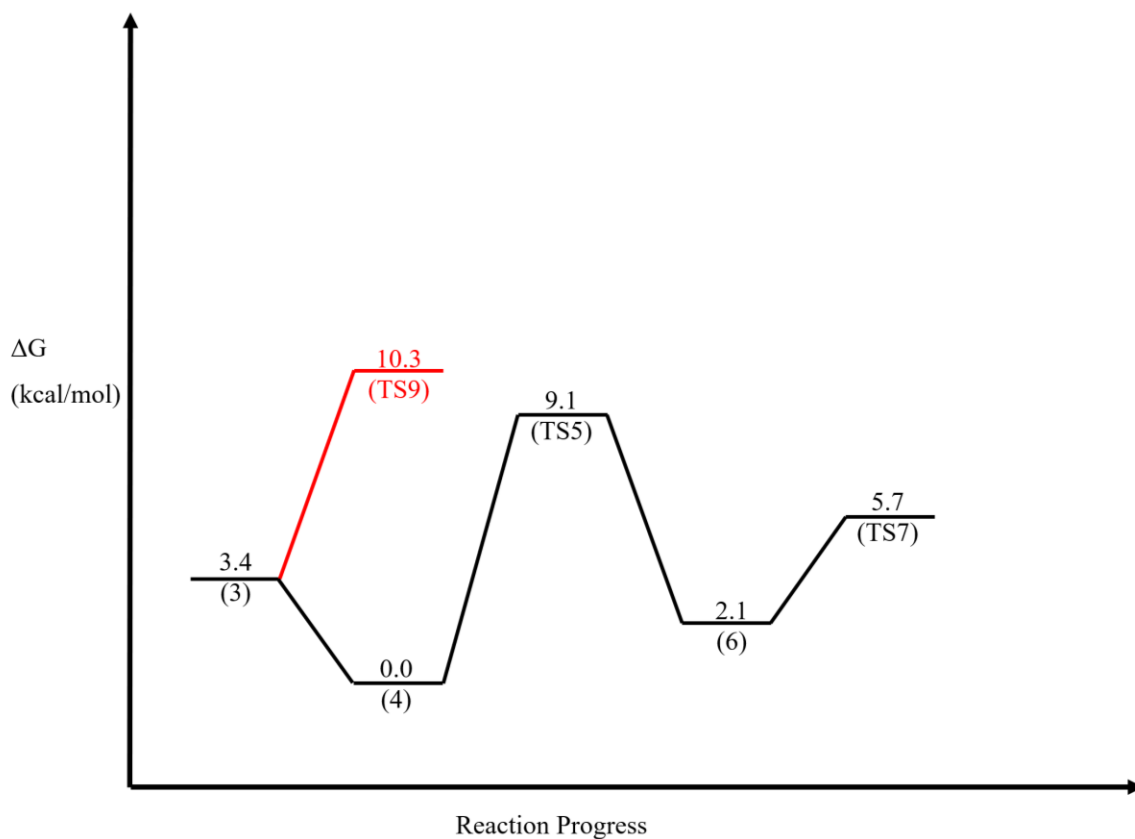


Figure 6. Visual reaction coordinate diagram for the 56-Linker.

The fourth monomer tested was the Two Ester Linker, indicating a relatively moderate reaction with an 80% conversion in 90 minutes under room temperature conditions (Park et al., 2016). The two ester computational results, displayed in Table 4 below, supported the experimental results in this case indicating a reaction in which polymerization was favored by about 1.6 kcal/mol. The polymerization and deactivation pathways did however have a high energy for activation with values of 20.5 kcal/mol and 22.1 kcal/mol respectively; however, the energy difference was slightly higher than the previous 56-Linker, meaning that the conversion or speed of the reaction should be greater in the Two Ester Linker than the 56-Linker. This further supported the experimental results previously found indicating the same conversion for both reactions, but a faster reaction with the Two Ester Linker than the 56-Linker. A visual depiction of the results is displayed below in Figure 8.

Table 4. The change in energy, enthalpy, and Gibbs free energy of the Two Ester Linker. All values are given in kcal/mol.

Step of Reaction	ΔE	ΔH	ΔG
3	5.0	5.4	2.3
4	0.0	0.0	0.0
TS5	6.4	5.7	7.4
6	5.0	6.2	6.2
TS7	21.5	20.3	20.5
TS9	12.9	13.1	22.1

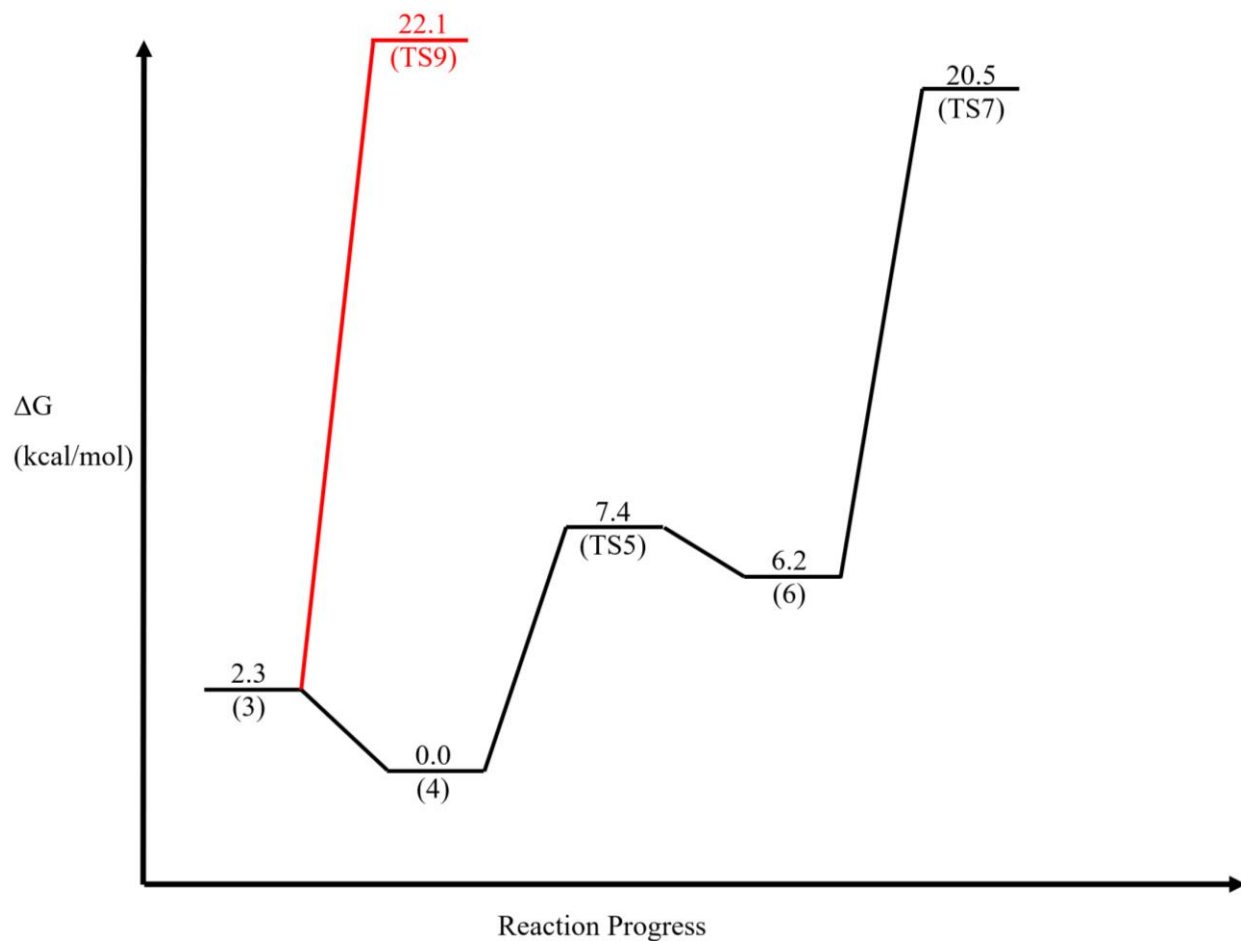


Figure 8. Visual reaction coordinate diagram for the Two Ester Linker.

The fifth and sixth monomers tested for computational values was the One Ester Linker conformers. This Linker was slightly different than the rest due to the diastereomeric identity that it contained. The one ester group can either be cis or trans to the hydrogen adjacent to its position and connecting to the cycloalkene portion of the monomer. The experimental results displayed no reaction for this solution, but each conformer of the One Ester Linker needed to be tested to compare to these results (Park et al., 2013).

The other test that needed to be conducted before going further for each conformer was to compare the (TS2) transition states for each monomer to compare the relative ratio in which they each react with the catalyst at any point in time. Since both diastereomer pair exists in solution,

the (TS2) transition state energy barrier will depict which monomer is favored for the catalyst to bind with at any point in time. The R conformer and the S conformer resulted in only a 0.2 kcal/mol difference being at 7.3 kcal/mol and 7.1 kcal/mol respectively. The negligible difference in energy required for each to bind with the catalyst meant that both would react relatively the same in reaction.

The R conformer of the One Ester Linker displayed a clear result indicating that the deactivation pathway would be followed in all cases that the catalyst would bind to an R monomer. The results displayed in Table 5 below indicate a relative activation barrier of only 17.3 kcal/mol for deactivation versus the 24.2 kcal/mol required for polymerization. The difference being -6.9 kcal/mol between polymerization and deactivation means that the deactivation pathway will always be followed. The results are visually depicted in Figure 9 below.

Table 5. The change in energy, enthalpy, and Gibbs free energy of the R conformer of the One Ester Linker. All values are given in kcal/mol.

Step of Reaction	ΔE	ΔH	ΔG
3	5.1	4.9	3.4
4	0.0	0.0	0.0
TS5	8.9	8.6	9.5
6	8.2	8.7	9.4
TS7	24.2	23.2	24.2
8	15.5	14.8	14.0
TS9	9.0	9.6	17.3

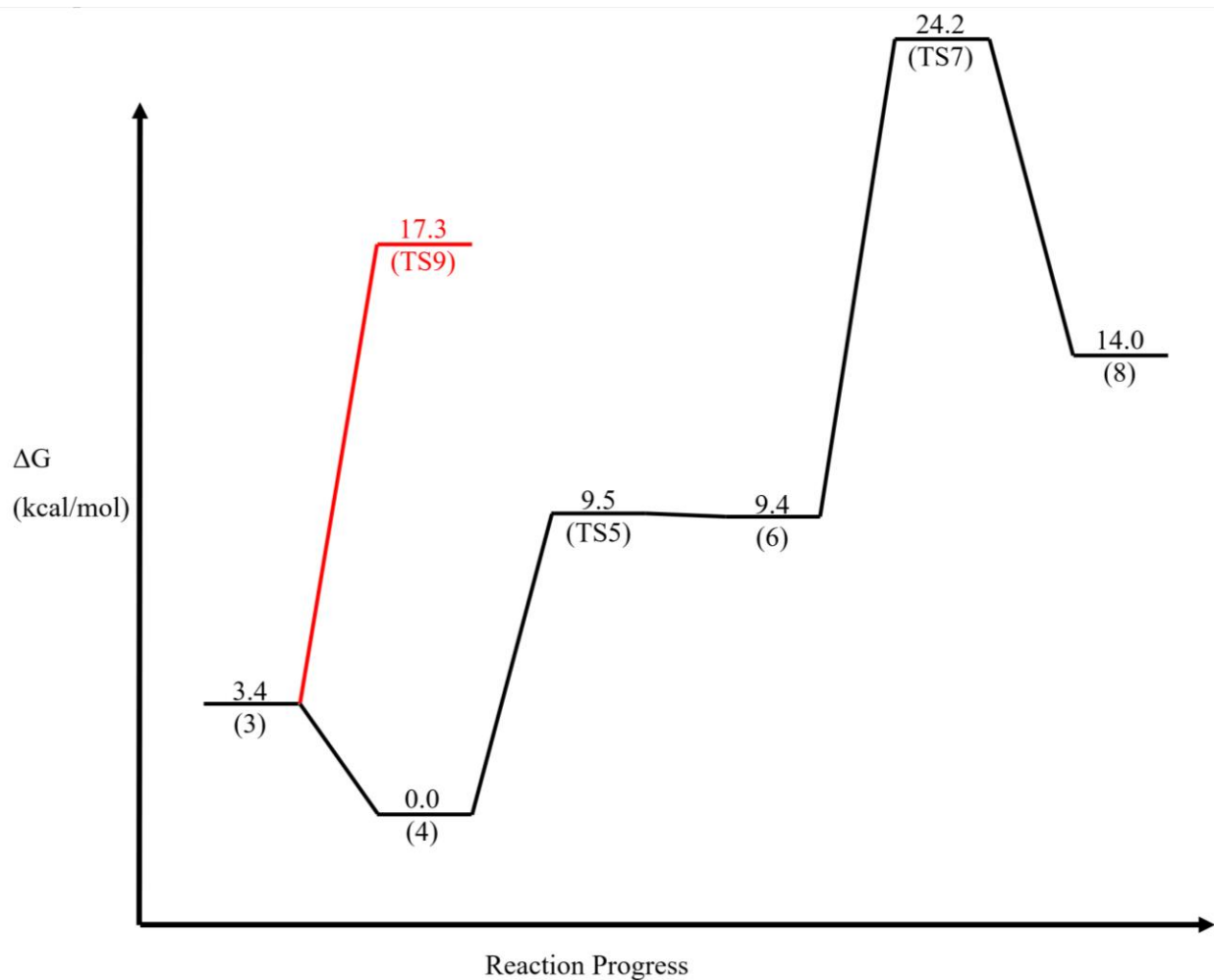


Figure 9. Visual reaction coordinate diagram for the R conformer of the One Ester Linker.

Before any conclusion can be inferred from the computational results, the S conformer of the One Ester monomer needed to be tested as well. The results indicated below in Table 6 display a relatively competitive reaction with a slight difference of only 0.5 kcal/mol favoring the polymerization pathway over the deactivation pathway. This meant that it would be a relatively 50:50 split between which monomers follow the deactivation pathway and which follow polymerization. The visual results are shown below in Figure 10.

Table 6. The change in energy, enthalpy, and Gibbs free energy of the S conformer of the One Ester Linker. All values are given in kcal/mol.

Step of Reaction	ΔE	ΔH	ΔG
3	4.0	3.6	2.2
4	0.0	0.0	0.0
TS5	6.6	5.8	6.3
6	5.3	5.4	5.5
TS7	14.2	12.9	13.3
8	9.1	7.3	6.7
TS9	5.3	5.7	13.8

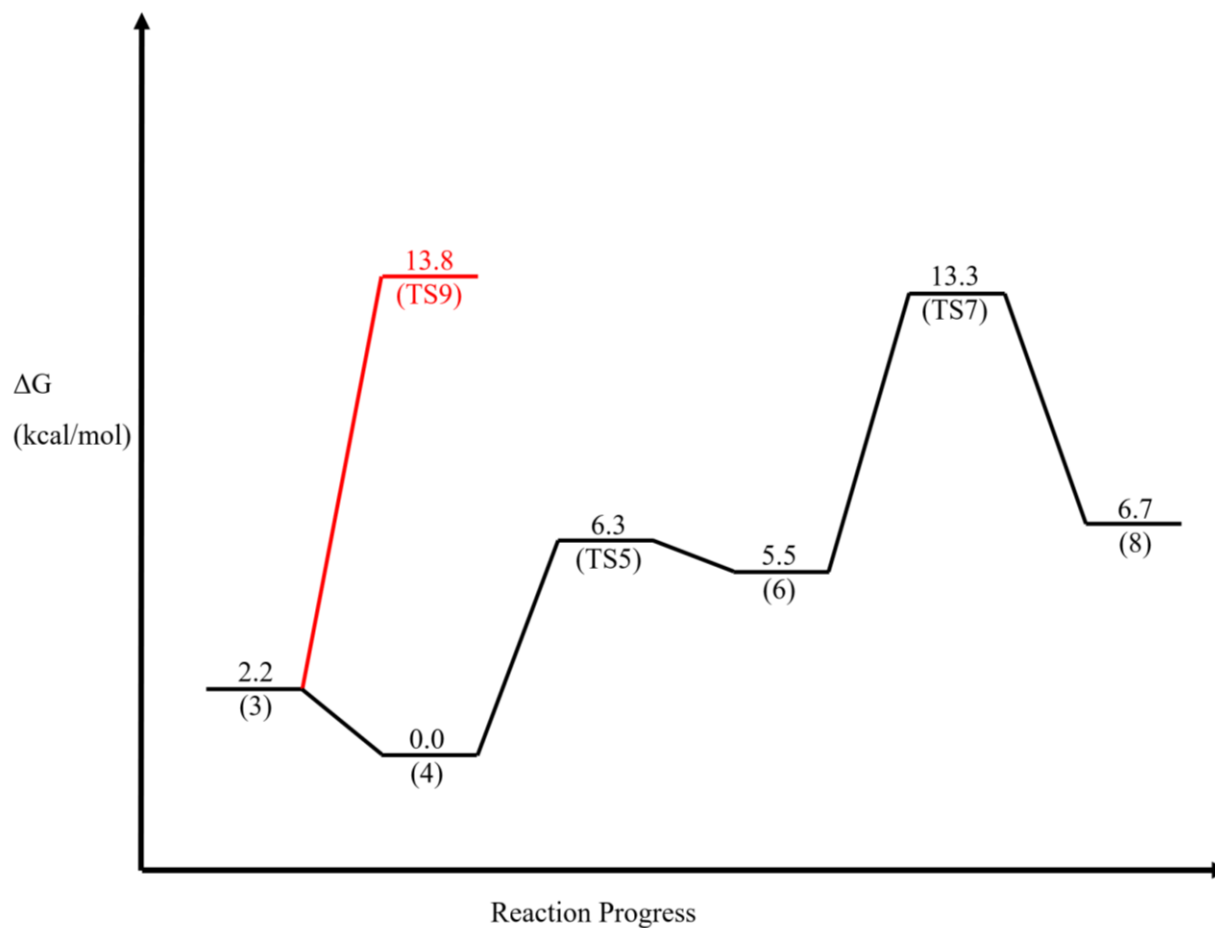


Figure 10. Visual reaction coordinate diagram for the S conformer of the One Ester Linker.

Combining the results from the R conformer and the S conformer of the One Ester Linker indicate a very minimal reaction being present or no reaction, further supporting the experimental results. The reason this was found is that it would be a relatively 3:1 ratio for deactivation or polymerization being followed for each catalyst undergoing the reaction pathway. About half of the catalysts will initially bind to the R conformer, resulting in all of them being deactivated. The other half of the catalyst will then bind to the S conformer, meaning that half of the them will be deactivated and half of them following polymerization. This means that 75% of the total catalyst during each step in the reaction will become deactivated. Statistically this would mean that the average polymeric length would be about 1.3 monomers linked together. The minimal chain length would indicate that no reaction would be present, supporting the experimental results.

The sixth monomer tested was the Oxygen Linker with previous experimental results indicating no reaction in solution (Park et al., 2013). The computational results verified the previous experimental results finding an extremely competitive reaction between both reaction pathways. The difference was negligible being only 0.1 kcal/mol increase for the polymerization pathway compared to the deactivation pathway. The relative energy barriers were 10.0 kcal/mol for the polymerization pathway versus 9.9 kcal/mol for the deactivation pathway. This meant that each pathway would be followed roughly half of the time, meaning that the average polymeric length would only be 1.9 monomer units in length on average. With such a small polymeric subunit, the reaction should be governed as having no reaction as any detection method will not be precise enough to be able to depict the small polymers. This means that the reaction will have no reaction in solution, further supporting the previously found experimental

results of the Oxygen Linker. A visual representation of the computational results is displayed below in Figure 11.

Table 7. The change in energy, enthalpy, and Gibbs free energy of the Oxygen Linker. All values are given in kcal/mol.

Step of Reaction	ΔE	ΔH	ΔG
3	2.0	1.2	-2.3
4	0.0	0.0	0.0
TS5	5.0	4.0	5.7
6	0.2	-0.1	0.9
TS7	10.5	8.9	10.0
8	5.4	4.0	3.5
TS9	3.8	3.6	9.9

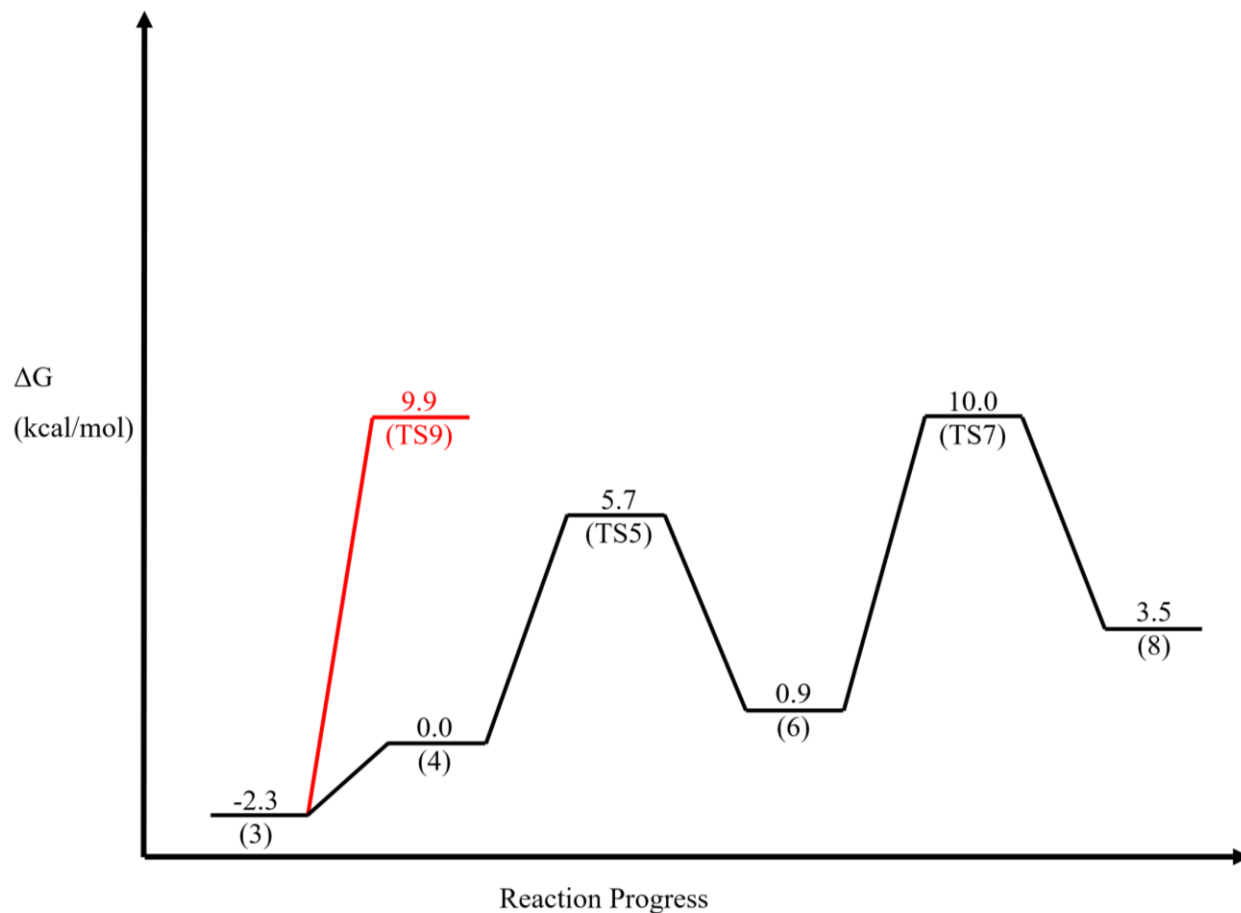


Figure 11. Visual reaction coordinate diagram for the Oxygen Linker.

After all the testing was completed, the goal of the research had still been unmet. Although the computational results had verified in most cases the experimentally found reaction outcome for each monomer, the results still did not provide an explanation for the reason why some monomers seem to be very favored to polymerize versus others seemed to deactivate and result in no reaction being present.

The answer lied in the visual analysis of the polymerization and the deactivation pathway steps. Since all compounds were relatively the same in shape and the only difference was the linker that had been used, the compounds that used this linker to alter the reaction progress were mainly analyzed. The polymerization pathway mainly did not have any interaction with the linker as it

was often pushed away from the reaction site and did not influence the reaction a great deal. The same could not be said for the deactivation pathway steps or more specifically (TS9). For this transition state, the linker comes into direct contact or is in the direct path of the second monomer that comes to bind with the catalyst from compound (3). The depiction of this step is shown below in Figure 12.

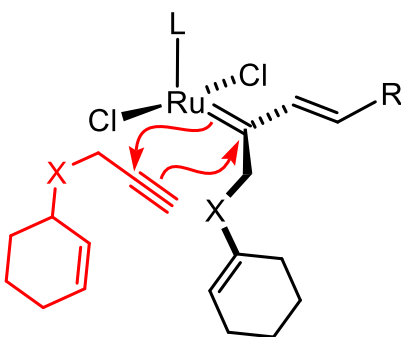


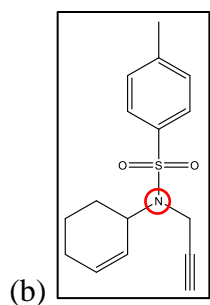
Figure 12. The (TS9) compound is shown for the deactivation pathway.

During this step in the reaction, the (X) generic linker is in the direct path of the second monomer, depicted in red, that binds to the active site of the ruthenium and carbon double bond. This meant that the greater this linker was at preventing this second monomer from binding, the greater the energy required would be for (TS9) to occur. Steric hindrance, or the ability for the relative size of an atom to repel other atoms from coming too close, was the most important or most influential factor then when determining if the reaction would occur. The greater the steric hindrance or relative size meant the more (TS9) was inhibited and the more polymerization would occur rather than deactivation.

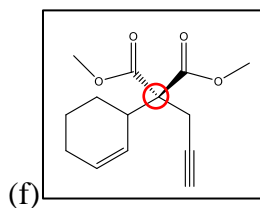
The steric hindrance effect would only be most influential when it would occur at the gamma position to the ruthenium atom. Every monomer had the linker at the gamma position except the 66-Linker and the 56-Linker which both had the OTs linker at the delta position to the

ruthenium. The gamma position in these cases were held by a small CH₂ group. This meant that although the large groups or the OTs linker were very large, they were not in the correct position to influence the (TS9) energy barrier as perfectly.

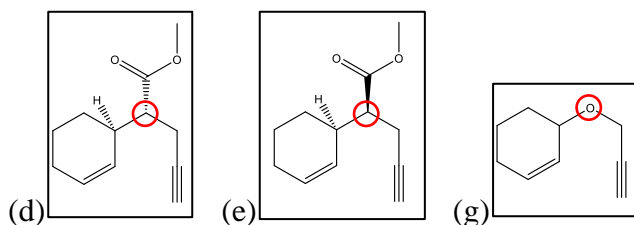
Using this conclusion, the monomers were ranked according by relative size or steric hindrance ability of the gamma carbon to the ruthenium as shown below in Figure 13. They were placed in four different categories. The first category having extremely high steric hindrance ability, meaning a very large group at the gamma position to the ruthenium atom. The second category was the moderate steric hindrance ability at the gamma position to the ruthenium. The third category was very little steric hindrance ability at the gamma position to the ruthenium. The final category was slightly different in that this category was one that included very little steric hindrance at the gamma position from the ruthenium atom but included a very large steric hindrance at the delta position to the ruthenium atom instead. The monomers were then compared to both the experimental and computational results shown in Table 8 below.



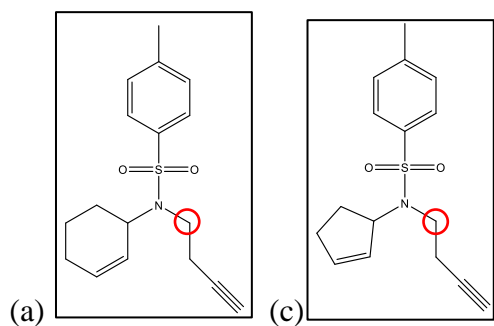
Category 1



Category 2



Category 3



Category 4

Figure 13. The monomers in categorical order. The monomers are the 66-Linker, the 65-Linker, the 56-Linker, the Two Ester Linker, the S conformer of the One Ester Linker, the R conformer of the One Ester Linker, and the Oxygen Linker from a to g respectively. Category 1 includes all monomers with a large steric hindrance at the gamma position to ruthenium. Category 2 include monomers with moderate steric hindrance. Category 3 include monomers with very low or no steric hindrance. Category 4 includes monomers with large steric hindrance at the delta position to the ruthenium atom. The gamma carbon to the ruthenium is circled in red.

Table 8. The experimental and computational results for the tested monomers. The computational results are displayed for both the quantitative results indicating the difference between the polymerization and the deactivation pathway and the quantitative results indicating the reaction predicted by the quantitative results. The predicted reaction is found by utilizing the steric hindrance ability by the monomer. The monomers are in the order depicted for the steric hindrance categories.

Results	Experimental (Conversion / time)	Computational (Quantitative) (kcal/mol)	Computational (Qualitative)	Predicted
b	100% / 1 minute	4.3	Fast	Fast
f	80% / 90 minutes	1.6	Moderate	Moderate
d	No reaction	-6.2	None	None
e	No reaction	0.5	None	None
g	No reaction	-0.1	None	None
a	30% / 12 hours	-0.6	None	Slow
c	80% / 12 hours	1.2	Moderate/Slow	Slow

The results shown in Table 8 indicate that the predictive method by using the steric hindrance ability can indicate the relative experimental results very proficiently, indicating the reaction outcome based on the steric hindrance for each monomer accurately. The computational results offer similar predictive ability, only not being able to indicate the reaction outcome in one monomer, monomer a. Moving forward from these results, the predictive ability of the monomers can be made into a generic model that the reaction progress follows. The inhibiting quality of the monomer can be depicted through Figure 14 below. In this predictive model, the steric hindrance ability of the monomer's linker governs the ability for the reaction to proceed.

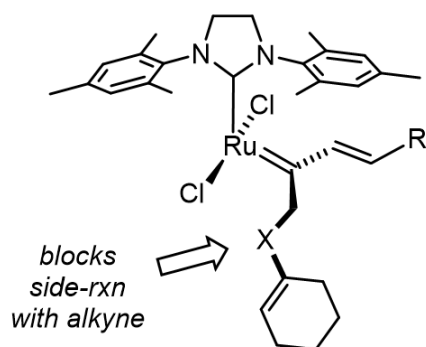


Figure 14. The generalized model predicting reaction outcome based on initial monomer steric hindrance ability.

Future Directions:

For future directions with this study, the generic predictive model should be tested. All tests of the generic model have indicated relative success for predictions based on steric hindrance. To verify these results, the 66-Linker should be modified to provide a 66-Linker isomer such that the OTs group is directly in the position of the gamma position for the ruthenium. This should promote the monomer from being in category 4 to being in category 1, changing the prediction from a slow reaction to a fast reaction like the 65-Linker. If the computational results can verify the predictive model, then it would be a verification regarding a proper functional predictive model.

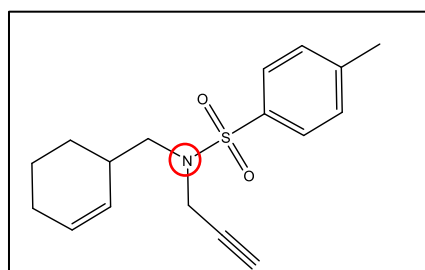


Figure 13. The newly created 66-linker isomer with the gamma carbon to the ruthenium in reaction is indicated.

Works Cited:

Park, H.; Lee, H.K.; Choi, T.L. Tandem Ring-Opening/Ring-Closing Metathesis Polymerization: Relationship between Monomer Structure and Reactivity. *J. Amer. Chem. Soc.* 2013. 135, 10769-10775.

Park, H.; Kang, E.H.; Müller, L; Choi, T.L. Versatile Tandem Ring-Opening/Ring-Closing Metathesis Polymerization: Strategies for Successful Polymerization of Challenging Monomers and Their Mechanistic Studies. *J. Amer. Chem. Soc.* 2016. 138, 2244-2251.